The Prediction of Cyclic Load Behaviour and Modulus Modulation for Polyester and other Large Synthetic Fiber Ropes.

C.M.Leech, S.J.Banfield, M.S.Overington, Tension Technology International Ltd and M. Lemoel SBM Inc.
36 Huggetts Lane
Eastbourne
Sussex BN22 0LU
England

***Abstract*- Fibre Rope Modeller (FRM) is a computer program for the analysis and prediction of synthetic fiber rope behaviour. It calculates the static tension-extension and torque-twist behaviour of fibre ropes using the basic fibre or yarn properties and the rope constructional parameters. It accounts for internal friction, internal polymer heating and material abrasion and fatigue to predict rope performance and life.**

This paper outlines the modulus modeling modifications recently made to FRM and describes how cyclic loading and its consequences are implemented into FRM. This paper also describes how the program has been validated using data from cyclic loading tests.

A full assessment of rope axial stiffness must include the effects of cyclic loading. Cyclic tension generates loops in the rope tension-extension plot. The area enclosed in these loops represents work done on the rope, and results in damping and hysteresis. For polyester ropes these loops do not follow the static tension-extension curve but a steeper curve; the analogy for this steeper curve is the unloading curve for post yield loading of steel. This steeper curve results in axial stiffening or modulus modulation, which produces a higher rope modulus than predicted by the static model.

FRM has been enhanced to use these material properties and to predict their effect on rope behaviour. These improvements now enable FRM to predict hysteretic damping, modulus stiffening and rope set caused by polymer residual strain. Further recent enhancements include the modelling of plaited and braided ropes, distortion and dilation of rope diameter due to bedding-in and creep strain.

1. INTRODUCTION

Background

The FRM computer rope program can model any textile structure eg yarns, strands, sub-ropes, and ropes, of twisted, laid or braided construction. It has been developed over the last twenty years, beginning with the original concept and code developed by Dr. C. Leech in the mid 1980s.

The first released implementation was Gen_Rope, developed by Tension Technology International (TTI) for the US Navy during 1988-93 as a DOS based program [1]. TTI then continued developing an enhanced version under the name to OpTTI-Rope and used that program for in-house and consulting work. A number of papers have been published describing that program [2,3,4,5].

With support of a UK Department of Trade and Industry grant [6], beginning in 2000, the program has now been converted to Windows and is being enhanced with many new features. This new Windows version, called Fibre Rope Modeller or FRM, is the topic of this paper.

Description of FRM

FRM describes the rope structure in much the same hierarchical manner that the rope is assembled. Figure 1 shows how a typical fiber rope is assembled. Basic yarns are twisted together to produce a rope yarn, a number of rope yarns are arranged in helical layers to produce a rope strand, and groups of strands are laid or braided together to form the finished rope.

The FRM modelling begins with describing a basic element, such as the fiber or basic yarn. Input data includes the basic element properties such as density, size, load-extension, break strength, friction, and coefficients for internal abrasion, axial compression, and hysteresis.

The way in which a group of such basic elements is assembled into the next hierarchical level is then described, number of elements, degree of twist, and variation of tensions. The assembly of a group of such elements into the next hierarchical element is then described, etc. Within each structural element, for example the strand, each component lower element, for example the rope yarn, follows a helical path about the central axis of that structural element, as shown in Figure 2.

FRM relates the tensions, extensions, torques and twists applied to the entire rope structure to those imposed on the hierarchical rope elements through the principal of virtual work. This can be stated simply that the overall sum of work performed on all elements of the rope is equal to the sum of the work performed by applying a tension which changes the rope length and the work performed by a torque which changes the rope twist.

Prescribed changes in length and in twist are applied to the rope. From the rope structural model, the resulting changes in length and twist on the next lower structural level are calculated. And from those changes, the succeeding changes in lower level elements are calculated, until the resulting change in length (stress) on the lowest or basic element is known.

The tension in the basic element which corresponds to this imposed change in length is calculated. Tensions and torques on each of the succeeding hierarchical elements are then calculated to determine the corresponding tension and torque on the rope itself.

In fiber ropes, the various structural elements can compress and change in shape. The resulting changes in diameter then alter the helical paths of succeeding levels and thus change other important properties.

The various elements can slip relative to each other. The degree of inter-element movement depends on the tension on an element, the pressure between elements, and the coefficient of friction. As a result of slippage, the balance of tensions between elements is changed, abrasion damage may be produced, and heat may be released.

Rope geometry

The modelling of structure geometry follows a hierarchical approach with a number of levels, which mirrors the manufacturing process. Typical sequences are filament, textile yarn, ropeyarn, strand, sub-rope, rope for a three strand rope construction illustrated in Fig. 1.

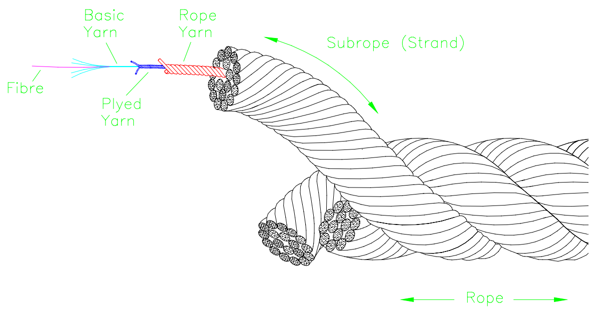

Figure 1. Typical components in a fiber rope

At each structural level (e.g., a strand), the next lower level form (e.g., the rope yarn) follows a uniform helical path around a central axis as shown in Fig. 2. This means that an individual filament will follow a complicated path determined by the multiplicity of helices. However, since the properties of each level are determined separately and used as input to the next higher level, these complications are avoided and the only geometry that needs to be defined is that of Fig. 2, with relations derived from the triangles in the "opened-out" diagram. The consequences on twist at a lower level of the subsequent twisting at a higher level have to be taken into account.

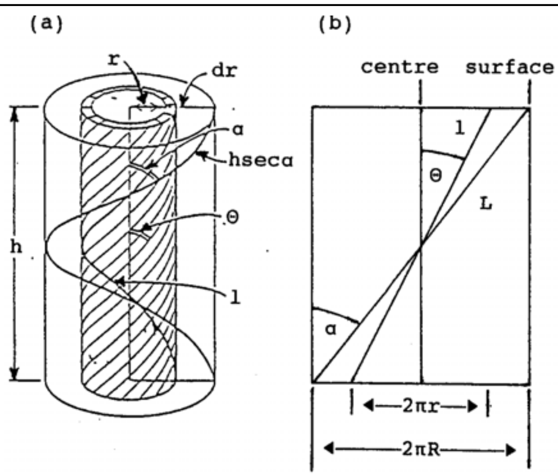

Figure 2. Twist geometry (a) components follow helical paths round concentric cylinders and (b) opening out flat defines geometrical and trigonometrical relations

Rope mechanics

The analysis is based on the Principle of Virtual Work:

P*L + **T***N = *__U__

where **P** is tension and **L** is elongation, **T** is torque and N is twist, and **U** is strain energy.
Because the rope is composed of an extremely large number of fine filaments, bending and torsional effects in the input components can be neglected. It is only necessary to take account of elongation energy obtained by integration of the tensile stress-strain properties, which can be measured on yarns in extension and recovery. Effects at higher levels come naturally into the analysis.

2. VERIFICATION OF FRM THROUGH TESTING

FRM was used to model a rope test conducted by Tension Technology International Ltd and SBM Inc., at National Engineering Laboratory (NEL) in November 2002. A subrope was removed from a 130mm diameter 5790kN minimum breaking load parallel strand polyester rope after 8 months use on the Girassol export buoy mooring. Testing of this 642kN minimum breaking load twelve strand subrope was conducted using the *Biharmonic* load profile develop by TTI Ltd and SBM Inc. [7] as shown in figure 3 ; this load profile is based around a pretension (approximately 17% of minimum breaking load as used in the mooring), second a periodic cyclic load overload and third a further cyclic load with different frequency and phase. The equation for this load profile is

$$T = T_p + a_1 \cos(\omega_1 t + \phi_1) + a_2 \cos(\omega_2 t + \phi_2)$$

where T is the applied rope tension, T_p is the rope preload {=985kN}, a_1 and a_2 are the two amplitudes {=30.768kN}, ω_1 and ω_2 are the two excitation frequencies {=0.51, 0.76 rad/s} and φ_1 and φ_2 are the two phases {=357° and 295°}.

The results of this test are captured in an Excel file and contains 9000 data points for time, rope tension and resulting strain.

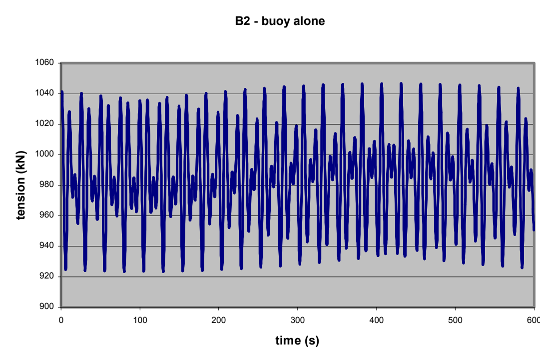

Figure 3. Biharmonic load profile

Description of rope

An outline of the sub-rope construction data for input into the model is included here for completeness, as follows:-
1 Each subrope is made from 12 strands, braided. Six of these strands migrate left (S) and six are right (Z)
3 Each strand is constructed from 899 textile yarns with a packing factor 0.8. The disposition of these yarns is in 18 layers and the layer population is 1, 6, 12, 19, 25, 31, 38, 44, 51, 57, 63, 70, 76, 82, 89, 95, 101 and 39
4 The diameter of the polyester textile yarn is 0.385mm, their tex is 110 corresponding to 0.11gm/m. The load extension behaviour is governed by a polynomial equation, as follows

$$L = L_b f(\eta) = L_b \left(a\eta + b\eta^2 + c\eta^3 + d\eta^4\right)$$

where L is yarn load, L_b is yarn breaking load (=71.978N), η is $\varepsilon/\varepsilon_b$, ε is the yarn strain and ε_b is the yarn breaking strain (=0.08). The coefficients a, b, c and d are 1.531,
-3.696, 6.894 and -3.729.

Figure 4 shows the modeled subrope load extension curve ; it is the static loading curve, referred to as the envelope.

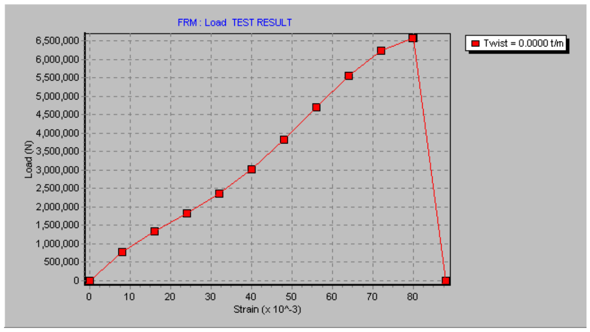

Figure 4 Subrope Load/Strain curve envelope

First the unloading typical in cyclic loading of polyester ropeyarns is considered.

Since polyester is used in this case, beyond its yield point which here is assumed zero, it behaves plastically. It unloads from a setting point along a different path to the load path, leaving the load envelope, Figure 5. If it is completely unloaded, it has a residual strain. On reloading it follows the latter (unloading) path until it reaches the setting point, and then follows the load envelope and acquires a new setting point.

Figure 5 shows the load envelope and the setting point, in this case at 0.5 normalized strain. In the vicinity of the setting point the modulus increases since the unloading path is steeper than that of the envelope. This results in a stiffening of the rope below the setting point, called modulus modulation.

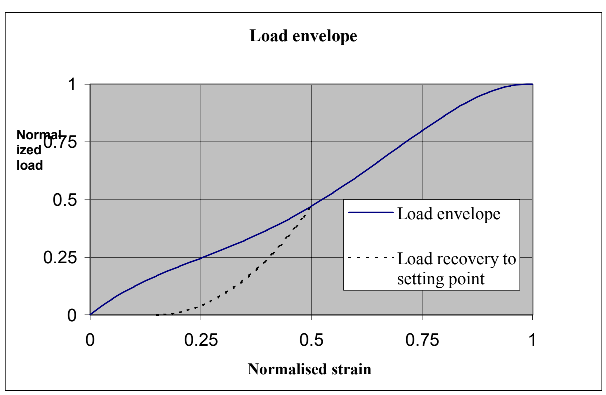

Figure 5. Load envelope in static and cyclic loading

To model the rope unloading behaviour it is necessary to use the modulus modulation properties of the basic fiber/ textile yarn as the rope code FRM uses fibre/textile yarn behaviour and the rope construction parameters to predict the rope behaviour. Accurate data for the unloading portion of the stress-strain envelope for the polyester fiber used in the tested rope was not available. Polyester data from a paper [8] by Casey was used to deduce this data, albeit it was for different grade of polyester. This data is then used in FRM to predict this specific rope behaviour. Another study [9] by Casey and Banfield showed that for a wide range of polyester grades and rope constructions typically offered for deepwater moorings, the COV (coefficient of variation in full scale rope axial stiffness falls within a narrow band of 5-8%. Thus, the use of a different grade of polyester is adequate to develop a typical set of coefficients for modeling in FRM. Clearly, for a given polyester grade, to ensure more accurate modelling, the coefficients must be established for the particular grade of polyester.

Second the strain rate effect is included in the above load strain function

$$
\begin{aligned}
L &= L_b f(\eta) \\
&= L_b\left(a\eta + b\eta^2 + c\eta^3 + d\eta^4\right) + \\
&\qquad \frac{\lambda L_b}{\varepsilon_b}\left(a + 2b\eta + 3c\eta^2 + 4d\eta^3\right)
\end{aligned}
$$

where λ is a strain rate parameter (~0.1sec) and is responsible for the hysteresis loops that arise in cyclic loading.

Results

The tests conducted at NEL are driven by rope load; this is programmed into the testing machine and applied to the subrope, which responds with an extension or strain. The Fibre Rope Modeller (FRM) on the other hand takes a given extension and determines the rope load. The NEL results were recorded in an Excel file with time (implied) in the first column, load and crosshead strain in the following columns; there are 9000 data points in this test accounting for 1800 seconds or 30 minutes. The subrope has been bedded in and relaxed to a 2% reference tension and the prestrain estimated to be ε_p=0.0089 (this value chosen to fit the predicted data at peak values) prior to these cyclic tests.

Figure 6 shows the crosshead strain measured in the subrope tests. The lower chart shows the complete data for 30minutes test time, 9000 data sets; the upper chart shows the strain time expanded so the behaviour of different strain amplitudes and rates can be seen. The full data set is shown to prove that this rope was fully bedded-in and that strain is not drifting up which always occurs during the bedding-in history of a rope. FRM has been modified to read those strain values, determine from them the strain rates and then to use the strain and strain rates to determine the subrope loads, which are then, compared with the NEL input data, Figure 7.

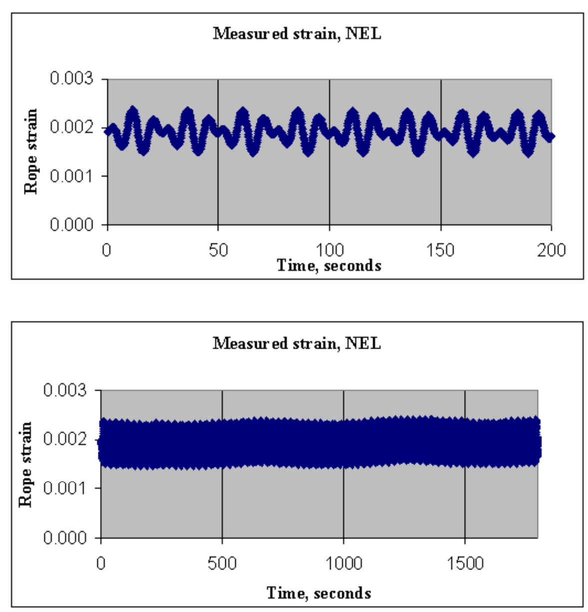

Figure 6 Measured crosshead strain at NEL (expanded time scale upper, 30 minutes for full test lower)

Figure 7 compares the loads predicted by FRM with the actual applied loads where a good fit can be seen. A better assessment of this can be realised by considering reduced data sets.

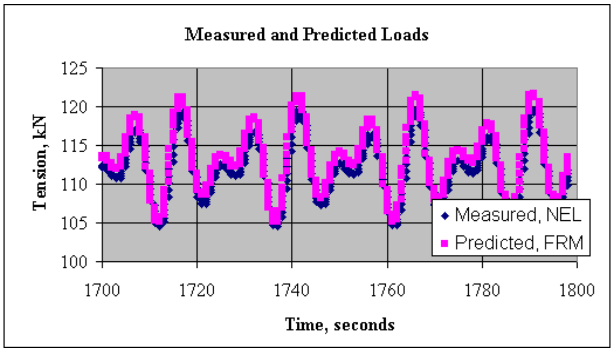

Figure 7 Comparison of measured and FRM modeled load

Figure 8 shows the first five hundred data points, 100 seconds and again shows that FRM has good agreement with that measured by NEL. The phase is not measurable here, implying a very small tanδ, although the lead between the load and strain is just discernible at say the 35sec time. The FRM data has been generated using λ=0.1 and recall that $\tan\delta = \omega\lambda$. The dilemma here is to select the frequency ω, there are two applied to the loading (biharmonic).

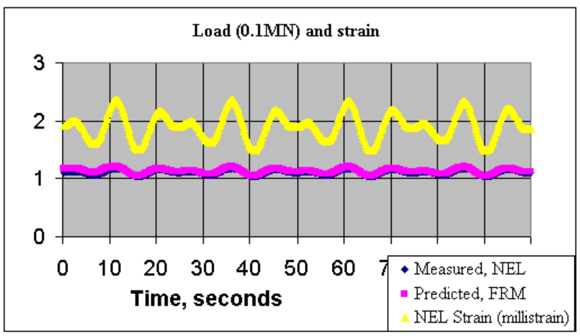

Figure 8 First five hundred data points

Figure 9 shows the last five hundred data points, 1700 to 1800seconds where good agreement is found.

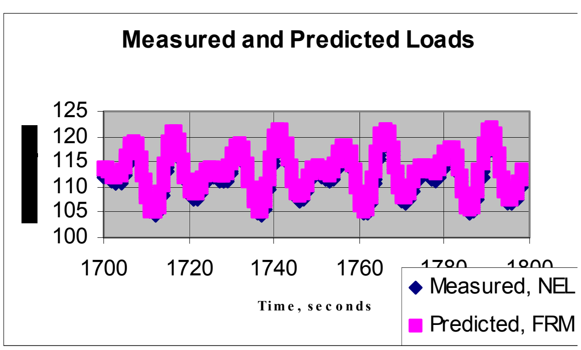

Figure 9 Last five hundred data points

Next, an analysis of axial stiffness for the small loadings in the region of 0.2 to 0.4% load range was conducted. This is an area of interest in load range for fatigue analysis where tens of millions of cycles occur in a fatigue spectrum. It should be noted that tension-tension fatigue is not a concern for the fibre rope, but is for the steel chain [10]. Since the loadings in a fibre mooring system are primarily derived from the polyester segments, the accuracy of axial stiffness is important. The modeling described herein has been used to gain a better determination of axial stiffness design values for fatigue.

Figure 10 shows the axial stiffness has been analysed using linear regression fits through the loading curve. Very high correlation coefficients were found showing consistency in the data. A comparison with the modeled data is also shown, again a good fit is shown in the X term which is the axial stiffness in kN. Note here that the ordinate is greatly expanded, and that the difference between predicted and recorded loads are only about 1.4%.

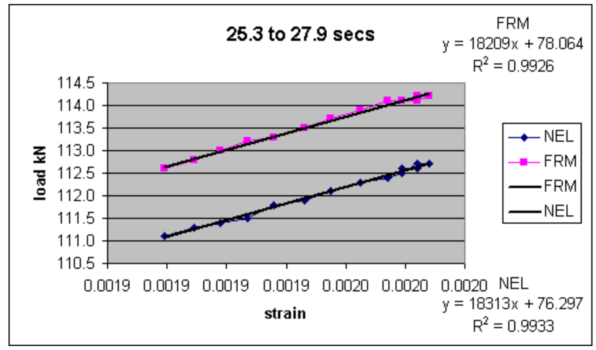

Figure 10. Axial stiffness analysis of raw data and comparison with modeled

A reasonable number of axial stiffness values at different times through the first 200 seconds of the test are summarized in table 1. The axial stiffness (EA) has been normalized by dividing by minimum breaking load (MBL) and is listed as EA/MBL. It can be seen that the FRM modeled data is very consistent as would be expected over the very narrow load range 0.2 to 0.4% with a coefficient of variation around 1%. The measured test data gave a high coefficient of variation around 6%.

Deduced from the modeling, axial stiffness is in the range of 28 to 29 compared to the test data which is in the range 28 to 33. Axial stiffness would be expected to be in the region of 1-3% coefficient of variation and not as high as 6%. Thus, it is apparent that the axial stiffness test values around 30 and higher are not real, but just artifacts from the complete measurement system in terms of load, strain and particularly the difficulty of detecting real strain in the rope as found by many researchers whether by optical or clamp on extensometers.

It has previously been proven [9] that axial stiffness increases with mean load and decreases with load range. At higher mean loads around 50%, axial stiffness typically does not exceed a peak value around 35 EA/MBL, thus the test values as high as 33 indicated by the test data are not possible at a mean load of 17%. Thus, axial stiffness in the range 28 to 29 indicated by FRM would be an appropriate upper bound design value for fatigue for a mean load of 17% of MBL.

seconds		Test load range %	EA/MBL		FRM/TEST % difference
From	to		FRM	TEST	
25.3		0.23	28.3	28.5	-0.7
50.3	52.3	0.23	28.9	29.7	-2.7
74.7	77.1	0.26	29	31.1	-6.8
99.9	102.1	0.3	28.3	31.8	-11.0
124.5	127.1	0.28	28.8	28.9	-0.3
149.5	151.9	0.39	28.1	33.1	-15.1
199.3	201.9	0.34	28.2	27.5	2.5
		mean	28.5	30.1	-5.2
		std dev	0.4	2.0	
		CV %	1.3	6.6	

Table 1. Comparison of axial stiffness modeled against measured

3. CONCLUSION

The TTI rope computer model program, FRM has been used to determine the behaviour of polyester fibre subrope.

a) The code was used to predict the rope loads for 9000 sequential strain data; these have been produced by 30 minutes of subrope cyclic testing (after a bedding-in sequence). The test profile was based on two frequencies over a static load.
b) The results show good agreement between the measured load (NEL) and the predicted load (FRM) for the complete 30minutes or 9000 data points for an 8 month used and bedded-in rope.
c) The predicted load extension curve for the strain cycles is in agreement with the measured curve.
d) For very small load ranges, axial stiffness values in the range 28 to 29 (EA/MBL) would be an appropriate upper bound design value for fatigue at a mean load of 17% of MBL
e) The hysteresis due to cyclic rate is not obvious. The near synchronous behaviour of the load and extension curves shows a small λ, strain rate effect, although the lead of the load is just discernible.
f) For small load ranges applicable to high numbers of fatigue loading cycles, the axial stiffness has a low coefficient of variation
g) Finally this has shown the benefit of using FRM to model cyclic behaviour of polyester ropes leading to more confidence in stiffness values for mooring system design.

Acknowledgements

The authors gratefully acknowledge the testing conducted by Robert Belshaw and analysis of subrope test data by Neil Casey at NEL. Also the work conducted by Cecil Melis at SBM in deriving the load spectrum for these tests. TTI gratefully acknowledges the support of SBM, Marc Lemoel, Robert Hobson, Jean-Loup Isnard and Benoit d'Hautefeuille

References

1. Fatigue Model of Aramid and Polyester Lines US Navy Contract N62474-87-C-3073, TTI (1992)
2. Hearle, J.W.S, Parsey, M.R, Overington, M.S, and Banfield, S.J 'Modelling the Long Term Fatigue Performance of Fibre Ropes', ISOPE, Singapore. July 1993.
3. Hearle, J.W.S, Hobbs, R.E, Overington, M.S, and Banfield, S.J, 'Modelling Axial Compression Fatigue in Fibre Ropes' ISOPE, 5th ISOPE The Hague June 1995.
4. Leech, C.M., Hearle, J.W.S.H., Overington, M.S., and Banfield, S.J.; 'Modelling Tension and Torque Properties of Fibre Ropes and Splices' ISOPE, Singapore. July 1993.
5. Banfield, S.J. and J.F. Flory, Computer Modelling of Large High-Performance Fiber Rope Properties, Oceans '95 Conference, MTS / IEEE, Piscataway, NJ, 1995
6. Performance prediction of Advanced Fibre Ropes Under Complex Loading Arrangements, Department of Trade & Industry funded project 27th March 2000 - 1st January 2004, by TTI, Marlow Ropes, Leeds University.
7. Methodology used to derive the HF components for stochastic rope testing, developed by C. Melis SBM Inc and S.J. Banfield TTI Ltd, dated 20th September 2002.
8. Short- and Long-Term Property Behaviour of Polyester Rope, Casey N.F, Belshaw R, Paton A.G. and Hooker J, Offshore Technology Conference, (OTC12177)
9. N.F. Casey, TUV NEL Ltd.; S.J. Banfield, Full-Scale Fiber Deepwater Mooring Ropes: Advancing the Knowledge of Spliced Systems OTC 14243, 2002
10. S Banfield, *TTI*, T Versavel, *Noble Denton*, RO Snell, *BP Amoco*, RV Ahilan, *Noble Denton* OTC 12175, May 2000, Fatigue Curves for Polyester Moorings - A State-of-the-Art Review